

# Susceptibility to bystander DNA damage is influenced by replication and transcriptional activity

Jennifer S. Dickey<sup>1,\*</sup>, Brandon J. Baird<sup>1</sup>, Christophe E. Redon<sup>1</sup>, Valeriya Avdoshina<sup>2</sup>, Guillermo Palchik<sup>3</sup>, Junfang Wu<sup>2</sup>, Alexei Kondratyev<sup>3,4</sup>, William M. Bonner<sup>1</sup> and Olga A. Martin<sup>1,\*</sup>

<sup>1</sup>Laboratory of Molecular Pharmacology, Center for Cancer Research, National Cancer Institute, National Institutes of Health, Bethesda, MD 20952, <sup>2</sup>Department of Neuroscience, Georgetown University, Medical Center, Georgetown University, Washington, DC 20057, USA, <sup>3</sup>Interdisciplinary Program in Neuroscience and <sup>4</sup>Department of Pediatrics, Georgetown University, Medical Center, Washington, DC 20057, USA

Received April 13, 2012; Revised July 27, 2012; Accepted July 30, 2012

## ABSTRACT

Direct cellular DNA damage may lead to genome destabilization in unexposed, bystander, cells sharing the same milieu with directly damaged cells by means of the bystander effect. One proposed mechanism involves double strand break (DSB) formation in S phase cells at sites of single strand lesions in the DNA of replication complexes, which has a more open structure compared with neighboring DNA. The DNA in transcription complexes also has a more open structure, and hence may be susceptible to bystander DSB formation from single strand lesions. To examine whether transcription predisposes non-replicating cells to bystander effect-induced DNA DSBs, we examined two types of primary cells that exhibit high levels of transcription in the absence of replication, rat neurons and human lymphocytes. We found that non-replicating bystander cells with high transcription rates exhibited substantial levels of DNA DSBs, as monitored by  $\gamma$ -H2AX foci formation. Additionally, as reported in proliferating cells, TGF- $\beta$  and NO were found to mimic bystander effects in cell populations lacking DNA synthesis. These results indicate that cell vulnerability to bystander DSB damage may result from transcription as well as replication. The findings offer insights into which tissues may be

vulnerable to bystander genomic destabilization *in vivo*.

## INTRODUCTION

The radiation induced bystander effect (RIBE) was originally described by Little and Nagasawa in 1992 in response to low dose alpha-particle radiation (1). They demonstrated that under conditions in which only 1% of a cell population was irradiated, 30% exhibited chromosomal changes. Thus, the RIBE has been defined as 'a cell's response to the fact that its neighbors have been irradiated' (2). Since that time, depending on the experimental set-up, various definitions have been proposed mainly reflecting inter-cellular communication (3). Bystander effects have been noted in response to a number of cellular stresses including other forms of ionizing radiation (IR), and non-IR sources of cellular damage (2,4–7). Recently, bystander effects were documented in response to media from tumor and aging cells (4). These findings have led to the notion that RIBE may be a specific example of a generalized population response to the presence of cells undergoing stresses of various types (8).

The consequences of the bystander effect include increased incidences of DNA damage, point mutations, sister chromatid exchanges, apoptosis and oncogenic transformation (2,5–6). Of these, one of the earliest recognizable effects in bystander cells is DNA double-strand

\*To whom correspondence should be addressed. Tel: +1 301 796 5028; Fax: +1 301 847 8512; Email: Jennifer.Dickey@fda.hhs.gov  
Correspondence may also be addressed to Olga A. Martin. Tel: +61 3 9656 1357; Fax: +61 3 9656 1424; Email: Olga.Martin@petermac.org  
Present addresses:

Jennifer S. Dickey, Office of In Vitro Diagnostics, Center for Devices and Radiological Health, Food and Drug Administration, Silver Spring, MD 20993, USA.

Olga A. Martin, Department of Radiation Oncology and Molecular Radiation Biology Laboratory, Peter MacCallum Cancer Centre and the University of Melbourne, Melbourne 8006, Australia.

break (DSB) induction (9–12). Phosphorylated histone H2AX (termed  $\gamma$ -H2AX) is a robust marker of DNA DSBs and has thus been utilized extensively to monitor bystander effect induction and signaling (9–11,13,14).

The mechanism through which bystander effects are propagated is not entirely clear, however several candidate molecules have been identified (2,6,15). Two of these molecules, nitric oxide (NO) and TGF- $\beta$ , have been causally linked to the RIBE as well as to bystander signaling from other forms of stress (4,16–18), suggesting that bystander signaling may utilize similar pathways regardless of the damage source.

One of the major questions remaining in the field is which cell types are vulnerable to bystander signaling. Clearly, some cell types are less sensitive to bystander effects (19). For instance, rapidly proliferating cancer cells in culture appear to be highly susceptible (16). This has led to some controversy in the field regarding the extent and even the existence of bystander responses (20). Previous studies have indicated that proliferating cells in S-phase are particularly vulnerable to bystander DNA DSB formation (21,22). However, other data suggest that S-phase is not the only factor determining bystander DNA DSB vulnerability (4,23). Identifying the cell types that may be vulnerable to bystander DNA DSB damage and possible genome destabilization is critical to understanding the importance of bystander damage in overall organismal health. Our hypothesis is that cell types with active DNA metabolism (i.e. high replication and/or transcription rates) may represent the cell population most vulnerable to bystander signaling. Thus, perhaps transcriptional as well as replicative status might determine which cell populations would be more susceptible to the formation of bystander DNA DSBs.

To test this hypothesis, we utilized two systems which contain non-replicating cells with various levels of transcriptional activity, primary rat brain cells and human lymphocytes. The brain contains distinct cell populations, representing both replicating (i.e. microglia and astrocytes) and non-dividing cells (i.e. post-mitotic neurons), that can be isolated and maintained in culture (24,25). Similarly, primary lymphocytes are normally metabolically inactive and non-replicating, but when activated, they first increase transcription levels and then begin to proliferate (26). Using these two model systems, we show that non-replicating bystander cells are still vulnerable to DNA DSB formation and document for the first time that ongoing transcription as well as ongoing replication may dispose cells to bystander signaling and ultimately genome destabilization.

## MATERIALS AND METHODS

### Primary microglial and astroglial cultures

Primary astrocytes and microglia were derived from 1- to 2-day-old Sprague Dawley (SD) rat (Charles River Laboratories, Wilmington, MA) cerebral cortices and cultured as described (27) with small modifications. In brief, the embryonic cortices were dissected, triturated and plated in tissue culture flasks that had been coated

with poly-L-lysine (75–150 kDa, Sigma-Aldrich, St Louis, MO). The cells were grown in Dulbecco's Modified Eagle's Medium/F12 (DMEM/F12, Invitrogen, Carlsbad, CA) supplemented with 10% fetal bovine serum (FBS) and 2% antibiotic-antimycotic solution (both from Invitrogen). The culture medium was replaced twice weekly. On day 6 of culturing, (6-days *in vitro*, DIV) the flasks were shaken at 100 rpm for 1 h. Supernatants were collected and centrifuged at 400  $\times$  g for 8 min. Microglial cells were resuspended in medium, replated and grown to confluence. Flasks then were continually shaken for 4 more days for collection of astrocytes. Cells were then trypsinized for 5 min, collected, and centrifuged at 400  $\times$  g for 8 min. The pellet was re-suspended in the proper amount of medium, plated and grown. The cells were cultured in tissue culture flasks, 6-well plates and LabTek II two-well chamber slides (Nunc, Naperville, IL). Cell culture details can be seen in (28).

### Cortical and hippocampal neuronal cultures

Rat cortical and hippocampal neuronal cultures were derived from embryonic (E) day E18 SD embryos and prepared and cultured as described previously (28) with minor modifications (29). Briefly, the embryonic cortices or hippocampi were cleaned from their meninges and/or blood vessels, minced and dissociated (30). The combined supernatants were centrifuged through a 4% bovine serum albumin layer (BSA, Invitrogen) and the cell pellet was resuspended in Neurobasal medium containing 2% B-27 supplement, 25  $\mu$ M Na-glutamate, 0.5 mM L-glutamine (all from Invitrogen) and 1% antibiotic-antimycotic solution. Cells were seeded at  $5 \times 10^5$  cells per ml on poly-L-lysine-coated tissue culture flasks, 6-well plates and chamber slides.

### Cerebellar granule cells

Cerebellar granule cells (CGC) were derived from postnatal day (P) 7–8 SD rats and cultured as described previously (31). Briefly, the meninges and blood vessels were removed from cerebella, and the cerebella were minced and dissociated. The cells were resuspended in Basal Medium Eagle (Invitrogen) containing 10% FBS, 0.5 mM L-glutamine 25 mM KCl and 1% antibiotic-antimycotic solution and seeded in poly-L-lysine coated tissue culture flasks, 6-well plates and chamber slides at  $5 \times 10^5$  cells per ml. Cytosine arabinoside (10  $\mu$ M; Sigma-Aldrich) was added 24 h after cell plating to inhibit glial proliferation. The neurons were cultured for 7 days before experiments started to assure all cells had reached a mature, terminally differentiated state. All cultures were incubated at 37°C in a humidified atmosphere containing 5% CO<sub>2</sub>.

### Lymphocytes

Human lymphocytes were isolated from whole blood obtained at the NIH Blood Bank. Blood samples were obtained from paid healthy volunteers who gave written informed consent to participate in an IRB-approved study for the collection of blood samples for *in vitro* research use. The protocol is designed to protect subjects from

research risks as defined in 45CFR46 and to abide by all internal NIH guidelines for human subjects research (protocol number 99-CC-0168). Blood was collected in lithium heparin tubes (BD, Franklin Lakes, NJ) and lymphocytes were separated using a Ficoll-Paque Plus gradient (GE Healthcare, Uppsala Sweden) (32). Cells were maintained in RPMI with Glutamax (Invitrogen) supplemented with 10% FBS and antibiotics (penicillin 100 U/ml and streptomycin 100 µg/ml) from Invitrogen. Either non-activated lymphocytes were used for experiments, or they were activated by incubation with 10 µg/ml phytohemagglutinin (PHA), 20 µg/ml lipopolysaccharide (LPS) and 5 µg/ml Concanavalin A (ConA, all from Sigma-Aldrich) for various times before the start of the experiments. All cultures were maintained in a humid atmosphere containing 5% CO<sub>2</sub>. To determine the effect of bystander signaling molecules on DSB induction in cells, 0–10 µM diethylamine NONOate (DEANO), 0–10 ng/ml recombinant transforming growth factor beta (TGF-β, both from Sigma-Aldrich) or 10 µg/ml TGF-β antibody (Promega, Madison, WI) was included in cell culture. In experiments to inhibit transcription, 10 µM α-amanitin (Sigma-Aldrich) was included in cell culture for 17 h prior to analysis.

#### Characterization of brain cell cultures

The brain cell cultures at 7 DIV were fixed in 2% paraformaldehyde and immuno-stained overnight at 4°C with antibodies (1:1000 dilution) against the following proteins:

- (1) Microtubule-associated protein 2 (MAP2; Millipore, Billerica, MA), as a neuronal marker;
- (2) Glial fibrillary acidic protein (GFAP; Abcam, Cambridge, MA), as an astrocyte marker;
- (3) Ionized calcium binding adaptor molecule 1 (Iba1; Wako, Japan), as a microglia marker;
- (4) Nestin (Abcam) as a neural stem cell marker (28).

The cells were then incubated for 1 h at room temperature with corresponding secondary antibodies (AlexaFluor 488 or 555; Molecular Probes, Eugene OR) in 1:1000 dilution followed by staining with 4',6'-diamidino-2-phenylindole (DAPI; Invitrogen) for 5 min. Microscopy was done using an Olympus IX-70 inverted microscope connected to an FV300 confocal laser scanning imaging system (Olympus, Center Valley, PA).

#### Medium transfer bystander methodology

The protocol is a modification of the medium transfer methodology for adherent cell cultures previously described (10). For adherent cell culture medium transfer protocols, dishes containing medium donor cell cultures with 90–95% cell density were chosen. For lymphocyte medium transfer, either quiescent, 17 h, or 36 h-activated cells were utilized. Cells were irradiated with 0.2 (rate of 0.45 Gy/min) or 20 Gy (rate of 11.24 Gy/min) γ-IR in a Mark-1 γ-irradiator (JL Shepherd & Associates, San Fernando, CA) or exposed to 100 J/m<sup>2</sup> UVC light generated with a UVLMS-30 EL Series 3UV lamp (UVP, San Gabriel, CA). Control samples were sham-irradiated.

The harvested medium (5 ml) was filtered through a 0.22 µm MILLEX<sup>®</sup>GP filter (Millipore, Billerica, MA) to separate the cells from the transferred medium and then added to recipient cultures after the original medium was removed and the cells were washed with PBS. The adherent medium recipient brain cells were seeded either onto Labtek II glass chamber slides 7 days prior to the experiment to ensure terminal differentiation. Controls for medium only and medium conditioned by recipient cell cultures were included in each experiment. The medium recipient cultures were incubated with transferred medium for various times (30 min to 24 h) before fixation in 2% paraformaldehyde in PBS for 20 min and staining. All time courses were performed at 37°C.

#### Co-culture bystander methodology

The protocol for co-culture experiments was as described previously (4). Brain cells were seeded onto LabTek II chamber slides at ~80% cell density. On the day of the experiment, the medium was aspirated, cells were washed with PBS and 200 µl of cold medium was added to the surface of the cells. Cells were placed on ice and aluminum foil was used to shield one-half of the cells. 100 J/m<sup>2</sup> UVC light was used to expose half the culture. Fresh warm media was then added to the cells and they were allowed to incubate from 30 min to overnight before fixation in 2% paraformaldehyde.

#### Cell mixing bystander methodology

The protocol for cell mixing experiments was a modification of the one previously described (10). CGCs obtained from a transgenic rat strain constitutively expressing GFP, SD-Tg(GFP)2BaIRrc P7 pups were plated into 2-well slides 7 days before the experiment (33,34). On the day of the experiment, the neurons at 50% confluency were either exposed to mock, 0.2 or 20 Gy γ-irradiation, or to 100 J/m<sup>2</sup> UVC light and intact CGCs were immediately added at the same concentration to the exposed cultures constitutively expressing GFP. The mixed cells were incubated for 24 h before fixation in 2% paraformaldehyde.

#### Immunocytochemistry and DNA DSB quantification

Lymphocytes were fixed, washed twice with PBS and then attached to slides through cytospin, after which both attached and suspension cells were processed similarly. For γ-H2AX staining, cells were washed in PBS and permeabilized in 70% ethanol pre-chilled to -20°C. Following blocking in 8% BSA for 1 h, the samples were incubated with anti-γ-H2AX mouse antibody (1:500, Abcam) for 2 h. Secondary antibodies were either anti-mouse Alexa Fluor-488 or Alexa Fluor-555-labeled antibody (Molecular Probes). Slides were then washed, mounted with propidium iodide (PI) or DAPI and viewed with a PCM2000 laser scanning confocal microscope (Nikon, Augusta, GA). Quantification of DNA DSBs, viewed as γ-H2AX foci was performed by manual counting with the microscope using a 100× objective, or counting foci in images. The number of foci was counted in ~100 randomly chosen cells in at least three separate

images. Alternatively,  $\gamma$ -H2AX intensity (reflective of foci density, the sum of pixels per nucleus occupied by foci) was determined in the brain cells using the Adobe Photoshop software package (Adobe Systems, San Jose, CA) as we described previously (35,36). These two measures are comparable. However, as found previously (35), due to the confounding nature of overlapping/touching foci, a more linear dose-response curve is obtained when analyzing foci intensity in the brain cells, as compared with the number of foci.

### Transcription analysis

Lymphocytes ( $3 \times 10^6$ ) or brain cells ( $1-3 \times 10^6$ ) were treated with  $20 \mu\text{Ci}$  [ $5\text{-}^3\text{H}$ ] uridine (Perkin-Elmer Life Sciences, Waltham, MA) for 3 h at  $37^\circ\text{C}$ . Total RNA was then isolated with the RNeasy mini kit according to the manufacturer's instructions (Qiagen, Valencia, CA). Radioactivity associated with RNA was counted by liquid scintillation spectrometry. Total [ $5\text{-}^3\text{H}$ ] uridine counts were normalized to the exact amount of cells in the samples. All experiments were performed three times in triplicate and the results are shown relative to quiescent primary lymphocyte cultures.

### Replication analysis

$\text{H}^3$ -conjugated thymidine ( $6.7 \text{ Ci/mmol}$ , ICN Biomedical, Costa Mesa, CA) was added to the cell media ( $0.5 \mu\text{Ci/well}$  in a six-well plate). Cells were incubated at  $37^\circ\text{C}$  for 24 h to allow sufficient time for uptake and DNA incorporation. After 24 h, cells were counted, trypsinized, and harvested and total genomic DNA was extracted using a genomic DNA preparation kit (Roche). The total radioactivity in the DNA preparation was determined by liquid scintillation spectrometry and the level of DNA replication was determined relative to astrocytes, which served as the positive control cell type. All experiments were performed in triplicate.

### Statistical analysis

Mean values were determined in at least four microscopic fields or in triplicate. Error bars show standard deviation or standard errors of the mean (SEM) as indicated. Statistical significance was determined using the student's *t* test. *P*-values  $<0.05$  were considered significant.

## RESULTS

### Replication and transcription levels in various cell types

Rat embryonic brain cells and human peripheral blood lymphocytes were examined. Five different brain cell populations were isolated from embryonic rats and maintained in culture: three neuronal types, cerebellar granular cells (CGCs), cortical neurons, and hippocampal neurons, and two non-neuronal types, astrocytes and microglia. A variety of markers was utilized to confirm the identity and purity of the different cell types in culture (Figure 1A).

The marker MAP2 belongs to a family of neuron-specific cytoskeletal proteins that are enriched in

dendrites, with a role in stabilizing dendritic shape during neuron development. The cortical, hippocampal and CGC cell populations exhibited MAP2 staining (Figure 1A, upper left image; CGCs shown). Another marker, nestin, is an intermediate filament protein expressed in dividing cells during the early stages of development in the central nervous system, peripheral nervous system, as well as in other tissues and is utilized as a marker of proliferating and migrating cells. The three neuronal cell populations lacked nestin staining (Figure 1A, upper right image; CGCs shown), indicating that these cultures lacked proliferating cells. During neuro- and gliogenesis, nestin is replaced by cell type-specific intermediate filaments, e.g. neurofilaments and glial fibrillary acidic protein (GFAP). GFAP, a protein marker for astrocytes was found to be absent in the CGC and hippocampal cell cultures, and present to a small extent ( $\sim 5\%$ ) in the cortical cell cultures (Figure 1B, left image; CGCs shown) and present in astrocyte cultures (Figure 1C, upper image). Iba1 (ionized calcium binding adaptor molecule 1), a 17-kDa protein specifically expressed in microglia (28) was also absent from the neuronal cell cultures (Figure 1B, right image; CGCs shown) but present in microglia cultures (Figure 1C, lower image). The presence or absence of these markers confirms that the hippocampal cell and CGC populations are free of contamination by the proliferating cell types, astrocytes and microglia.

DNA and RNA synthesis rates were measured in cultures of the five cell types. While the astrocytes and particularly the microglial cells exhibited substantial rates of DNA synthesis (Figure 1D, black bars and numbers), the CGC and hippocampal cell cultures lacked detectible DNA synthesis, indicating that these populations were terminally differentiated. The cortical cell cultures did exhibit a low level of DNA synthesis consistent with the level of astrocyte contamination observed microscopically. This contamination which did not exceed 5% of the total cell population could be eliminated from consideration in microscopy experiments as the two cell types could be distinguished based on cell size and morphology. Overall, these results confirmed that the neuronal cell preparations were terminally differentiated.

RNA synthesis was also examined with particular reference to those cell types that were found to lack DNA synthesis (Figure 1D, gray bars). Of the brain cell types, CGC cultures exhibited the most transcription, considerably above the level found in stimulated lymphocytes (Figure 1D, rightmost bars) shown for comparison. The other brain cell types exhibited rates of transcription between those of quiescent and stimulated lymphocytes (Figure 1D, gray bars and number).

### Bystander DNA damage in brain cell cultures

Cultures of the five types of brain cells were examined for their ability to exhibit  $\gamma$ -H2AX foci under two bystander scenarios. In the first, donor cultures were subjected to either 0.2 or 20 Gy IR. After 3 h, the media from these cultures were removed, filtered and added to duplicate unirradiated cultures. Both a low and high dose of

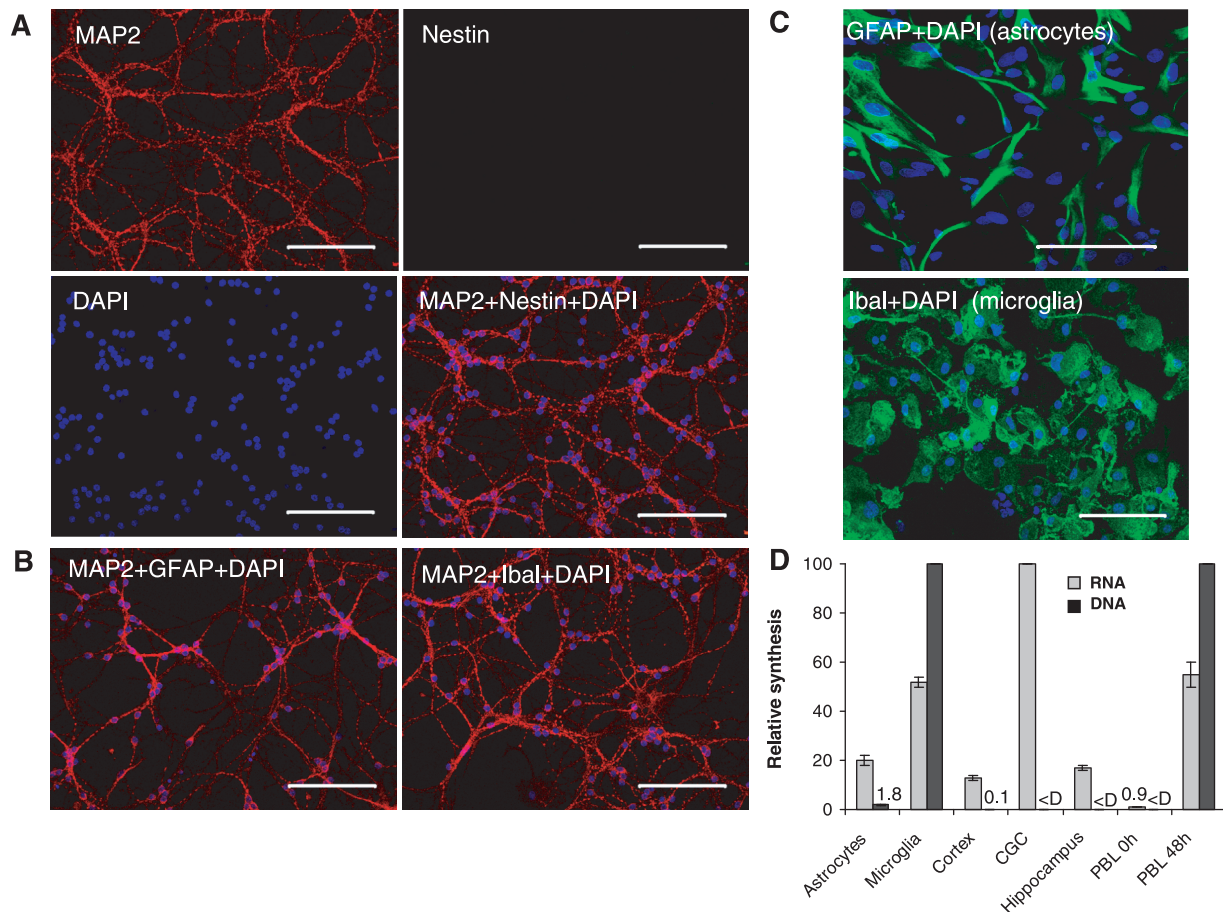


**Figure 1.** Characterization of brain cell types after 7 days in culture. Astrocytes, microglia, cortical neurons, CGCs and hippocampal neurons were obtained and cultured as described in Materials and Methods. (A) Representative images of CGC cultures stained for MAP2, a neuronal marker (red), Nestin, a neural stem cell marker (green) and DAPI for DNA (blue). The CGC cultures stain positive for MAP2 and negative for Nestin, confirming that they are non-proliferating and terminally differentiated. (B) Representative images of CGC cultures stained for MAP2 (red), either GFAP, an astrocyte marker (left, green) or Ibal, a microglial marker (right, green) and DAPI (blue). The cultures stain negative for GFAP and Ibal, indicating they are free of astrocyte and microglial contamination. (C) Positive control images of astrocytes (above) and microglia (below) stained for GFAP or Ibal (green), respectively, and with DAPI (blue). Bar = 100  $\mu$ m. (D) Relative DNA (black bars) and RNA (gray bars) synthesis in brain cell cultures were measured by 24 h  $^3$ H-thymidine (microglia set to 100) and 3 h  $^3$ H-uridine (CGC set to 100) incorporation, respectively. Included for comparison relative DNA and RNA synthesis in Peripheral Blood Lymphocytes (PBL) at either quiescence (PBL 0h) or 48 h after activation (PBL 48h) measured by 24h edU (L 48 set to 100) and 3 h  $^3$ H-uridine incorporation, respectively. Error bars are the standard deviation of three experimental replicates done in triplicate.

$\gamma$ -radiation were selected to see if a dose response would be detected in these cell types or if the typical ‘all-or-nothing’ bystander DNA damage response would be observed (11). Treatment with UVC light was also chosen because it causes thymine dimers and not DSBs in exposed cells, while bystander DNA DSBs can be observed in neighboring cells (37). The  $\gamma$ -radiation doses used here were utilized in previous studies and may help to uncover similarities and differences between low and high dose  $\gamma$ -radiation with UVC (10,38–40). In both cases, the amount of  $\gamma$ -H2AX expression was measured in the bystander cells after various time intervals (Figure 2).

In contrast to  $\gamma$ -or X-ray irradiation which generates relatively homogenous discrete foci, irradiation by UVC induces a wide variety of cell cycle dependent  $\gamma$ -H2AX staining ranging from foci to nucleus-wide pan-staining of various intensities (41). Cells in S-phase exhibit a nuclear-wide bright staining that is consistent with

replication blockage (by thymine dimers or by other aberrant structures appearing during DNA repair) while cells in G1 exhibit no or small increases in  $\gamma$ -H2AX that are associated with NER intermediates (41). Increase in  $\gamma$ -H2AX is observed in UV-damaged G1 cells if repair by NER is compromised (41). In agreement with these reports, UVC irradiation of neurons showed no statistically significant increase in  $\gamma$ -H2AX foci at early time-points (in the few hours after treatment). However, after 1 or 2 days, exposure to UVC results in a fraction of cells that have high levels of  $\gamma$ -H2AX that spreads widely in the nucleus (pan-stained cells) (Figure 3A). These cells are believed to be associated with the induction of apoptosis.

The bystander astrocytes and microglia exhibited substantial DNA damage, 3–4-fold and 8–10-fold over the controls, respectively (Figure 2A, top panel). With IR, elevated  $\gamma$ -H2AX levels were apparent by 1h, reached a

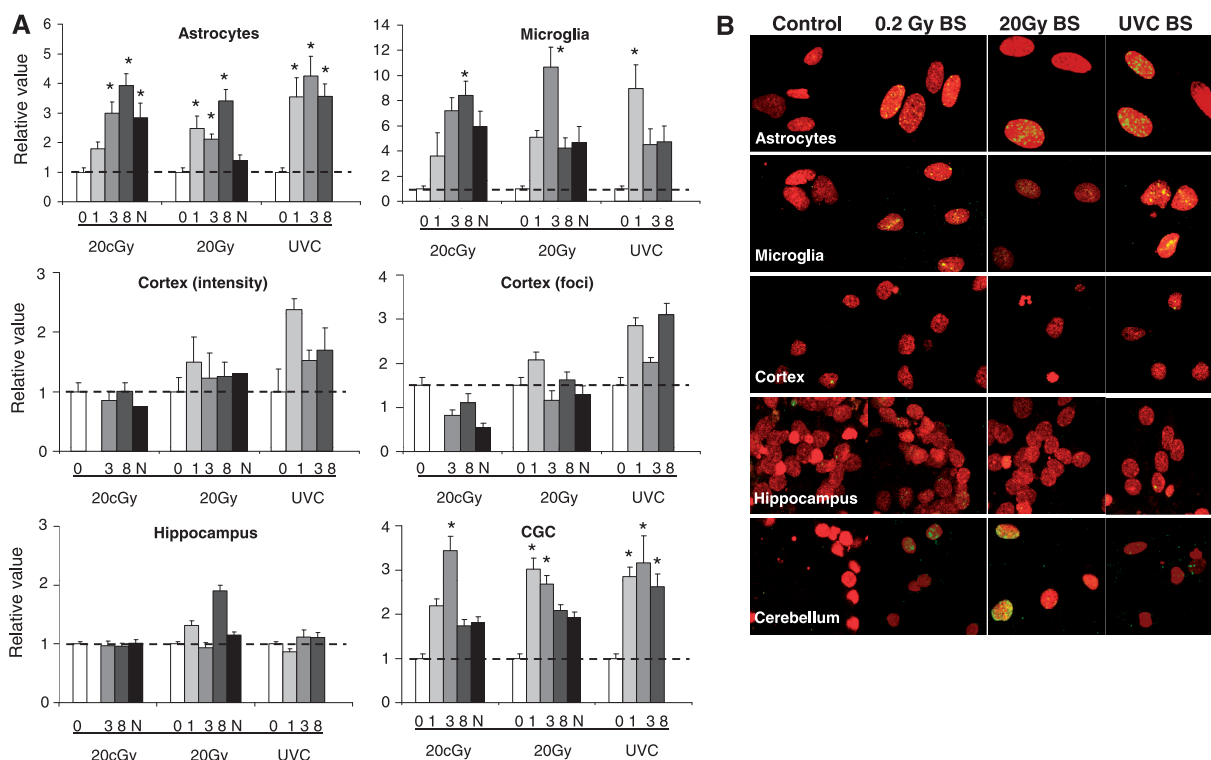


**Figure 2.** Bystander effect in brain cells. (A) For IR, cultures of astrocytes, microglia and cells from the cortex, cerebellum and hippocampus were subjected to either 0.2 or 20 Gy of IR. After 3 h, the media was removed, filtered and placed on duplicate but unirradiated cultures of the same cell type. For UVC, one-half of the cell cultures were covered with aluminum foil during irradiation with 100 J/m<sup>2</sup>. Cultures were fixed at various times post-addition as noted (0 control, 1, 3, 8 or N, overnight). Each panel displays the average increase in  $\gamma$ -H2AX intensity per cell type. The average  $\gamma$ -H2AX intensity per nucleus was measured as described in Materials and Methods. As a crosscheck, the cortical cultures were also analyzed by manual foci counting. Consistent with our previous reports (35,36), the two methods gave comparable results (middle two panels). Error bars represent the standard error of the mean for at least 100 cells. (B) Representative images of bystander cell cultures are shown for each cell type (rows) and each treatment (columns). Asterisks show significant differences from control values,  $P \leq 0.05$ .

maximum at 3–8 h, persisting overnight. With UVC the kinetics were more rapid with a maximal or almost maximal response at 1 h. Both these cell types undergo DNA synthesis, thus the finding that they exhibit substantial bystander  $\gamma$ -H2AX levels serves as a positive control. The images in Figure 2B are representative of the  $\gamma$ -H2AX response in bystander cell populations.

Of the three neuronal cell types, only the CGC cultures consistently exhibited bystander  $\gamma$ -H2AX formation, in amounts similar to that found in astrocyte cultures. The cortical and hippocampal cell cultures exhibited little or no bystander  $\gamma$ -H2AX, possibly because they exhibited levels of transcription less than 15% of the CGCs. As previously mentioned, the small amount of DNA synthesis observed in the cortical cell culture was found to be due to contamination by astrocytes. These astrocytes were not included in the cortical cell bystander data.

To confirm that CGC cultures exhibit bystander DNA damage independent of the method, a mixed culture protocol was also examined. Cultures of GFP-expressing CGCs were exposed to 0.2 Gy, 2 Gy IR or 100 J/m<sup>2</sup> UVC. Immediately after exposure, normal CGCs were added to the exposed cultures and incubated for at least 24 h to allow the added cells to attach (Figure 3). Foci were counted in both the exposed and bystander cells. Bystander cells 1 day after mixing exhibited 1.5–2-fold

increased  $\gamma$ -H2AX foci over the controls and lower values after 2 days. These values are consistent with those obtained in previous experiments in which IR induced 2-fold increased levels of  $\gamma$ -H2AX in bystander samples after overnight incubation.

These results with CGCs indicate that certain cell types that lack DNA synthesis may exhibit bystander DNA damage, possibly due to a high level of transcription. Thus, transcriptional complexes may also be vulnerable to bystander DNA damage in addition to DNA replication complexes.

### Bystander signaling in lymphocytes

Human peripheral blood lymphocytes are quiescent with low endogenous transcriptional activity when isolated (26). However, when stimulated, cultures exhibit increasing levels of RNA synthesis beginning 5 h after activation but do not exhibit detectable levels of DNA synthesis until after 24 h (Figure 4A). Thus, there is a time interval when these cultures exhibit substantial transcription without DNA replication between ~5 and 20 h after activation.

Cultures stimulated for 17 h as well as quiescent cultures were examined for their abilities to exhibit bystander DNA damage. The images in Figure 4E are representative of the  $\gamma$ -H2AX response in media transfer protocols

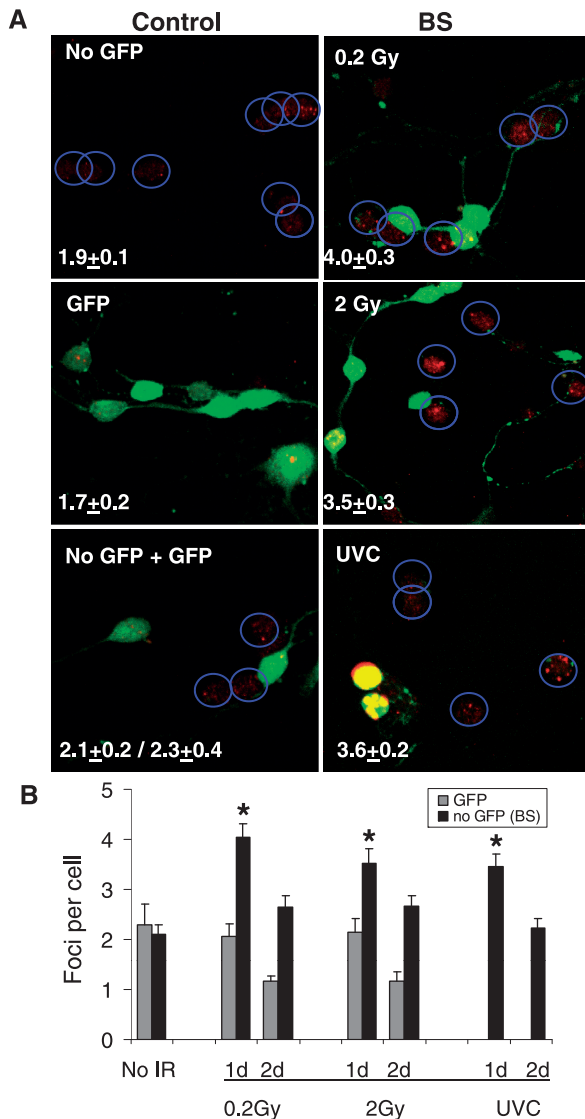


**Figure 3.** CGC bystander effect with normal and GFP-expressing CGCs in mixed cultures. (A) GFP-expressing CGCs (green) were irradiated with 0.2 Gy, 2 Gy IR or UVC, then mixed with non-GFP expressing bystander cells and cultured for 24 h. Cultures were fixed and stained for  $\gamma$ -H2AX (red). The nuclei of the CGCs not expressing GFP are noted by blue circles. Numbers of  $\gamma$ -H2AX foci per cell were calculated and the values shown in the lower left corner of each image. (B) Average numbers of  $\gamma$ -H2AX foci per cell after various treatments are compared at 1 day and 2 days incubation of irradiated and unirradiated cells. Values for bystander cells (no GFP, black bars) are compared with values in directly irradiated cells (GFP, gray bars). Error bars represent the SEM for at least 50 cells in four microscopic fields. Asterisks show significant differences from control values,  $P \leq 0.05$ .

compared with direct exposure. Quiescent and 17 h activated lymphocytes responded similarly to direct exposure to IR and UVC (Figure 4B and C, gray bars), indicating in both cases that similar amounts of DNA damage were inflicted and that DNA DSB detection was operative.

However, the bystander responses were substantially different in the two types of cultures. Quiescent bystander

cells had a weak DNA damage response to media from quiescent cultures irradiated with IR or UVC (Figure 4B, black bars) and also to media from activated cultures exposed to UVC (Figure 4D). In contrast, the 17 h activated cultures responded to media from both quiescent and activated cultures exposed to either IR or UVC (Figure 4C and D), although media from quiescent cultures exposed to 0.2 Gy induced a considerably weaker response that duplicate cultures exposed to 20 Gy.

In each case, recipient quiescent cultures responded less robustly to bystander signaling compared with recipient stimulated cultures. However, media from both stimulated and quiescent exposed cultures induced substantial increases in  $\gamma$ -H2AX levels in activated cultures, indicating that while quiescent lymphocytes may not respond to bystander signals, they are capable of generating signals similar in strength to those from stimulated lymphocytes. Because the lymphocyte cultures were taken well before the onset of DNA replication, these results indicate that active transcription in non-proliferating cells may make them vulnerable to bystander DNA damage.

#### The effect of transcription inhibition on bystander DNA damage induction in non-proliferating cells

If transcriptional activity predisposes non-replicating cells to bystander effect vulnerability, then inhibiting transcription should mitigate bystander induced increases in  $\gamma$ -H2AX. This prediction was examined utilizing  $\alpha$ -amanitin to inhibit RNA synthesis.

In lymphocytes (Figure 5A), the presence of  $\alpha$ -amanitin in the recipient cultures of 17 h stimulated lymphocytes (pre-DNA synthesis) prevented the induction of  $\gamma$ -H2AX levels by media from irradiated lymphocytes. Similarly, in CGCs (Figure 5B) the presence of  $\alpha$ -amanitin in the recipient cultures reduced the bystander  $\gamma$ -H2AX induction. When  $\alpha$ -amanitin was also present in the media of the donor CGC culture prior to IR exposure (and was thus carried to the recipient culture during media transfer), the bystander  $\gamma$ -H2AX induction was reduced  $\sim$ 2-fold. Thus inhibition of transcription in the recipient cultures was effective in mitigating bystander  $\gamma$ -H2AX increases, indicating that it is the ongoing transcriptional activity is the primary factor that predisposes these cells to bystander DNA damage. That inhibition of transcription in the donor exposed cultures also mitigated bystander  $\gamma$ -H2AX increases may be expected since signal induction in the donor cells may also require transcription.

#### The effect of TGF- $\beta$ and NO on DNA damage induction in non-proliferating cells

TGF- $\beta$  and NO have been implicated in bystander response signaling (42). These molecules lead to increased levels of  $\gamma$ -H2AX similar to those observed in bystander effect studies. Also anti-TGF- $\beta$  has been reported to mitigate bystander responses (16,17). With lymphocytes, the extent of  $\gamma$ -H2AX increase depended on the state of the cultures (Figure 5C). Quiescent lymphocyte cultures (L Q) did not respond to media from irradiated lymphocytes, as expected, and also did not respond to either TGF- $\beta$  or the NO generator DEANO (DNO). Pre-S stimulated

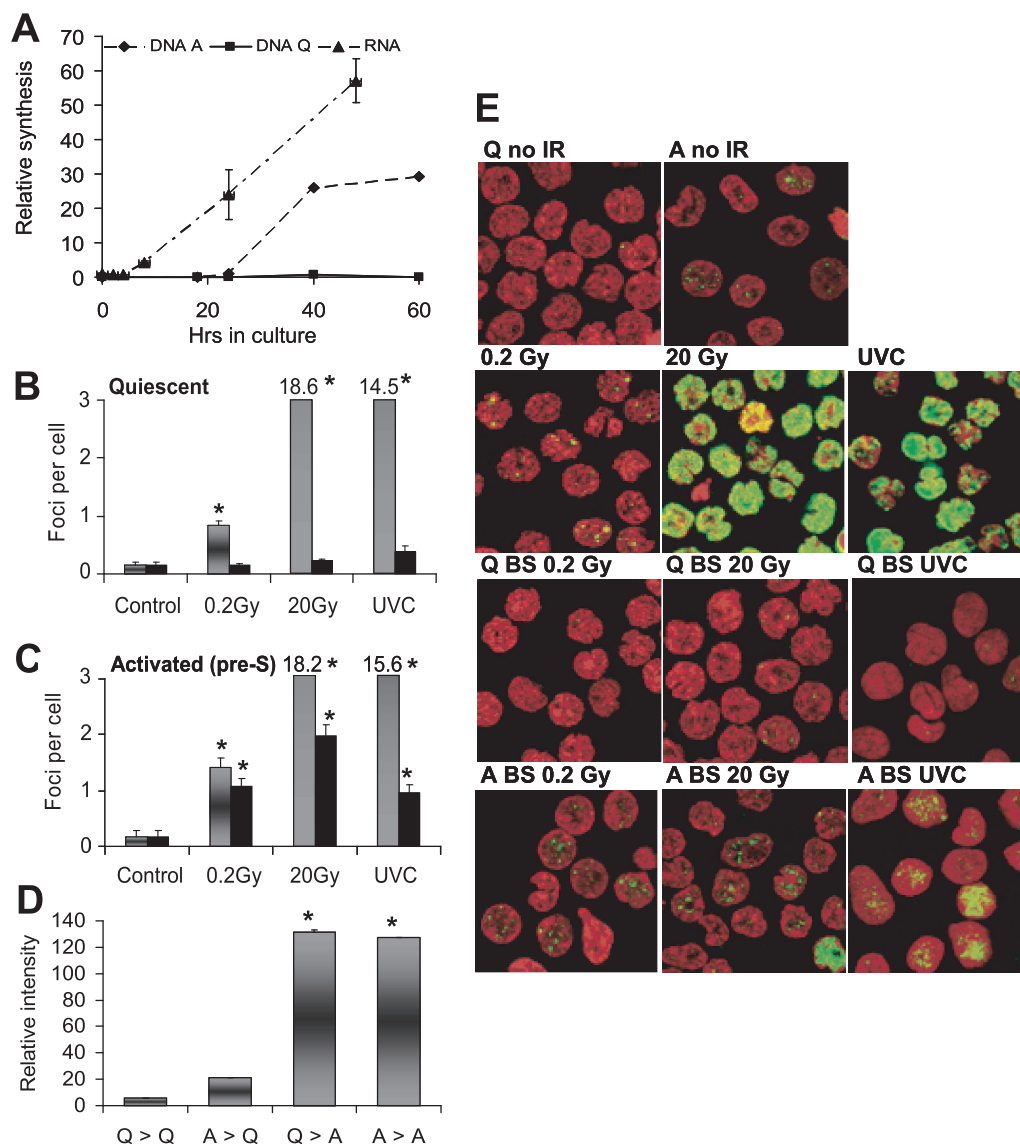


**Figure 4.** Bystander responses in lymphocytes. (A) Rates of RNA (triangles, [ $^3\text{H}$ ] uridine incorporation) and DNA (diamonds, edU incorporation) synthesis were determined for times after activation in primary human lymphocytes. Squares indicate DNA synthesis in quiescent lymphocytes for reference. Although increased RNA synthesis was apparent 5 h after activation, DNA synthesis was not detectable until after 20 h. Lymphocytes activated for 17 h were used in these experiments. Error bars represent the standard deviation of three independent experiments. The average numbers of  $\gamma\text{-H2AX}$  foci per cell in directly exposed (gray bars) or bystander (black bars) lymphocytes are shown after exposures to 0.2 Gy, 20 Gy or 100 J/m $^2$  UVC. Lymphocytes were quiescent (B) or activated for 17 h (C). Error bars represent the SEM for at least 100 cells in four microscopic fields. (D) Media was transferred 3 h after exposure from UVC-irradiated quiescent cells to bystander quiescent cells (Q > Q), from UVC-irradiated activated cells to bystander quiescent cells (A > Q), from UVC-irradiated quiescent cells to bystander activated cells (Q > A) and UVC irradiated activated cells to bystander activated cells (A > A). Error bars represent the SEM for at least 100 cells in four microscopic fields. (E) Representative images from the experiments shown in (B) and (C). Nuclei are stained with PI (red) and  $\gamma\text{-H2AX}$  foci are shown in green. The first two rows show irradiated cells and the bottom two rows depict bystander cells (BS). Asterisks show significant differences from control values,  $P \leq 0.05$ .

lymphocytes (L 1dA), while responding to media from irradiated lymphocytes, appeared not to respond to TGF- $\beta$  and only slightly to 10  $\mu\text{M}$  DNO. S-phase lymphocytes (L 2dA), stimulated for 36 h, responded to both TGF- $\beta$  and DNO with elevated  $\gamma\text{-H2AX}$ .

With CGCs, there was considerable elevation in  $\gamma\text{-H2AX}$  levels in response to media from irradiated CGCs as well both TGF- $\beta$  and DNO (Figure 5C, right set of bars). The  $\gamma\text{-H2AX}$  levels induced by the two molecules were similar to that by media from irradiated CGCs.

These results support the notion that bystander  $\gamma\text{-H2AX}$  levels are induced in non-proliferating actively transcribing cells through mechanisms similar to those reported for proliferating cells.

## DISCUSSION

Bystander effects have been found in cell populations in response to a number of different types of stress including radiation, UV exposure and even tumor

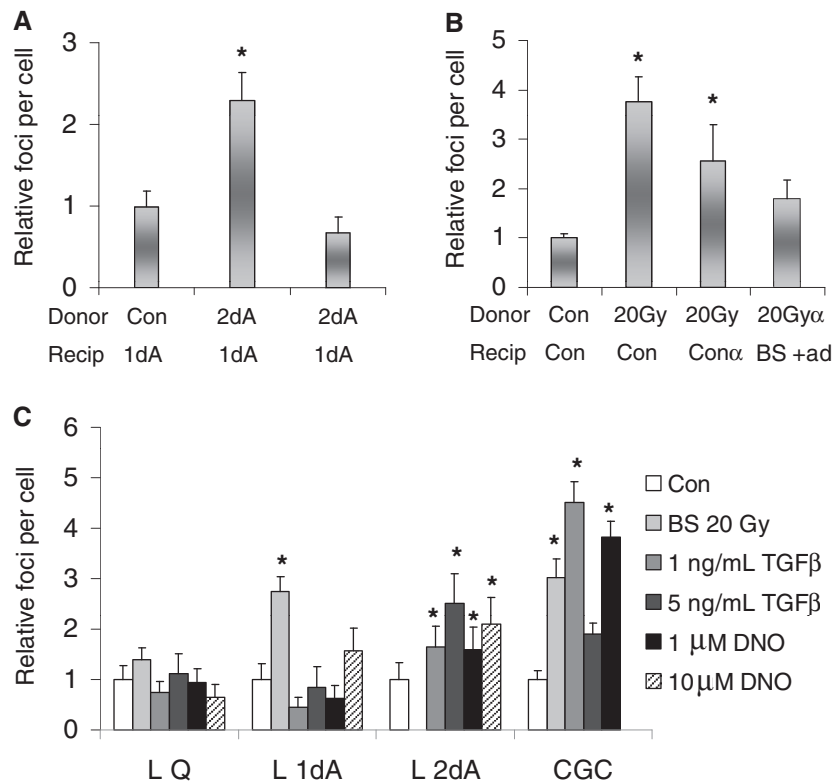


**Figure 5.** Factors affecting bystander responses. Inhibition of transcription lessens bystander effect signaling in lymphocytes and CGCs. (A) For lymphocytes, donor cultures were activated for 36 h (2dA), by which time DNA synthesis was present (Figure 4A). Media was transferred to cultures activated for 17 h (1dA), before DNA synthesis was ongoing. As noted,  $\alpha$ -amanatin was added to the recipient bystander lymphocytes (1dA $\alpha$ ). (B) For CGCs, donor CGCs were exposed to 20 Gy, and after 3 h the conditioned media was transferred to recipient bystander cultures. As noted,  $\alpha$ -amanatin was added to the recipient bystander CGCs (Con $\alpha$  in recipients) or donor cultures (20 Gy $\alpha$  in donors). (C) TGF- $\beta$  and NO can mimic bystander effects. The  $\gamma$ -H2AX foci numbers are shown for cultures of quiescent (L Q), 17 h-activated (L 1dA) and 36 h-activated (L 2dA) lymphocytes as well as cultures of CGCs incubated in the presence of TGF- $\beta$  or the NO generating compound DEANO at the concentrations noted. The values are compared with those obtained with media from cultures subjected to 20 Gy (BS 20 Gy), with the exception of L 2dA cultures. Error bars represent the SEM for at least 100 cells in four microscopic fields. Asterisks show significant differences from control values,  $P \leq 0.05$ .

presence (2,5–7,37,38,43). One important consequence of bystander signaling is the induction of DNA DSBs in bystander cells because these are known to induce genome destabilization (9–12). DSB induction is a serious challenge for cells requiring repair and increasing the risk of genomic instability, mutation and transformation, it is essential to understand bystander signaling (13,44). In particular, understanding the cell types that are vulnerable to this effect as well as the mechanistic basis of its propagation would greatly enhance our ability to predict the impact of this effect on overall organismal health.

Previous research has shown that replicating cells are particularly vulnerable to the bystander effect (4,21,23). However, our and others' work have demonstrated that cells in S-phase are not the only susceptible cell populations (4,45). In this study, we showed that two types of non-proliferating cells, terminally differentiated neurons and primary lymphocytes, respond to bystander signaling if they exhibit substantial transcriptional activity. Figure 6 summarizes the correlations we obtained between DNA and RNA synthesis levels and vulnerability to several sources of bystander signaling.

Two types of neuronal cells, from the cortex and hippocampus, did not exhibit detectible bystander responses and were also largely unresponsive to TGF- $\beta$  or NO. In contrast, CGCs, non-replicating cells, which displayed substantial transcription levels, were responsive to both bystander signaling and the external application of the putative bystander signaling molecules TGF- $\beta$  and NO. These results indicate for the first time that, in addition to active DNA replication, transcriptional activity is an indicator of bystander effect vulnerability.

Primary human lymphocytes are quiescent but after stimulation in culture, there is a time interval where they increase transcription levels about 10-fold but lack replication (26). During this interval, the lymphocytes respond to bystander signaling. The fact that  $\alpha$ -amanitin treatment alters bystander responses even after activation indicates that the transcriptional activity itself, rather than other factors, is the important determinant of bystander vulnerability in non-proliferating cell populations. Recently quiescent lymphocytes exposed to media from irradiated cells were shown to develop increased micronuclei post-activation. This article also indicated that ROS might be an element in bystander signaling (46). These

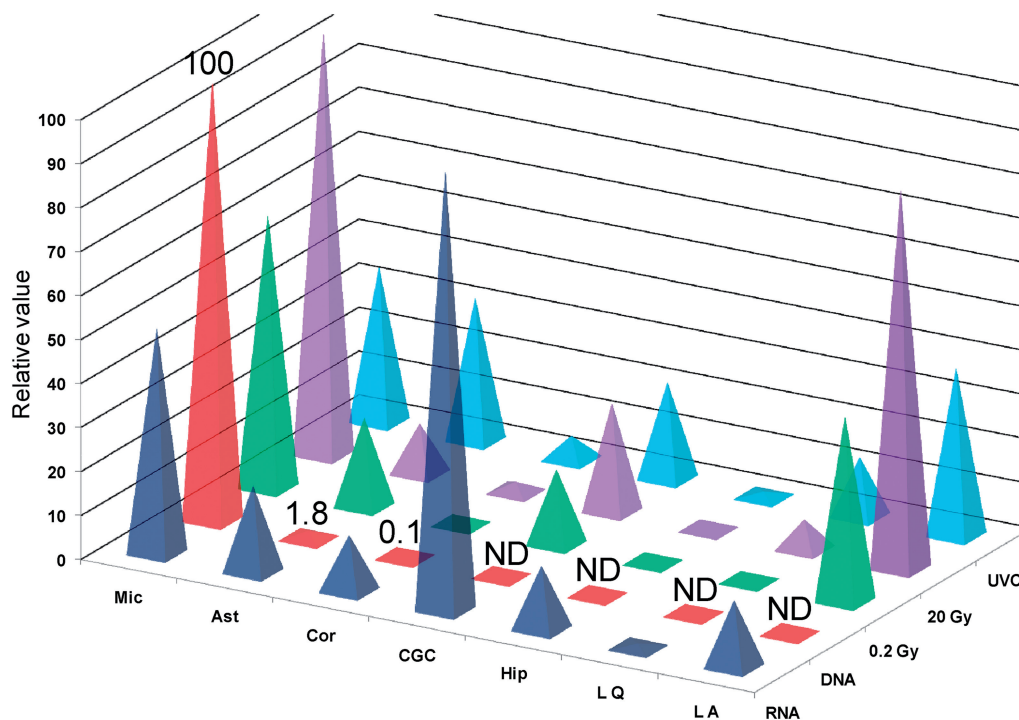


**Figure 6.** Relative magnitudes of bystander effects in cultures of lymphocytes and brain cells correlated with their levels of DNA and RNA synthesis. Mic, Microglia; Ast, Astrocyte; Cor, Cortex; Hip, Hippocampus; LQ, Quiescent lymphocytes; LA, Activated lymphocytes; ND, Not detectable.

data support the notion that non-replicating cells may be impacted by the RIBE.

The neonatal mouse cerebellum has been demonstrated to be a valuable model to study RIBE *in vivo* (47). When radiosensitive *Patched-1* (*Ptch1*) heterozygous mice were subjected to the X-ray irradiation of their bodies while their heads were protected, increased levels of DSBs, apoptosis and tumor formation were found in the unirradiated cerebella. The mechanisms behind long-range 'bystander' responses are still largely unknown, however several hypotheses have been proposed in recent years. Intercellular signalling molecules such as TGF- $\beta$ 1 and nitric oxide originating from irradiated cells have been shown to play a major role in transferring the damage signals to bystander cells (16,37). Furthermore, COX2, the protein kinase-C family, the PI3-related kinases ATM/ATR and the mitogen-activated protein kinase (MAPK) pathways seem to have a pivotal role in bystander processes (see Baskar for review) (48). Although the same factors may be involved in the RIBE *in vivo*, other mechanisms engage the gap junction intercellular communication (GJIC) for transmission of bystander signaling. GJIC was shown to be critical for transmission of oncogenic radiation damage to the bystander cerebellum in mice through connexin43 upregulation and the release of ATP (49,50). However, it is reasonable to suppose that *in vivo*, RIBE may be also mediated by factors diffusing through both gap junctions and the bloodstream. As CGCs are sensitive to exogenous oxidative stress (51), these cells are good target for the RIBE *in vivo*.

In bystander cells, it is believed that NO and TGF- $\beta$  mimicking inflammation-induced ROS ultimately lead to

different types of DNA damages including non-DSBs (clustered DNA lesions among others) and DSBs lesions (10,52,53). In replicative bystander cells, DSBs are thought to occur when DNA replication forks collide with structures originating directly (i.e. single-strand breaks) or indirectly (i.e. irreversible topoisomerase cleavage complexes) from oxidative DNA lesions (54). Similarly, it is realistic to think that a transcription fork interfering with an oxidative DNA lesion can lead to DSB formation (Figure 7). In fact, several recent studies show the presence in both replicating and non-replicating cells of transcription-mediated DSBs (55–57). In neurons, these DSBs result in ATM activation and  $\gamma$ -H2AX formation (55). Transcription-mediated DSBs might occur spontaneously in normal neurons in response to endogenous oxidative DNA alterations (58,59) and such DSBs may be one factor implicated in neurodegenerative diseases (60). Support for this notion comes from recent demonstration of DSB formation following activation of ionotropic glutamate receptors in mature, terminally differentiated cortical neurons *in vitro* (35) and in adult neurons following excessive excitation (seizures) in rat brain *in vivo* (36). Finally, we show here a similar response in bystander cells to low and high  $\gamma$ -irradiation and demonstrate that non-replicating bystander cells have typical 'all-or-nothing' bystander DNA damage (11).

Taken together, our results indicate that a number of cell types in the body could potentially respond to bystander signals and that the induction of  $\gamma$ -H2AX foci in response to TGF- $\beta$ , as well as basal transcription rates might be good predictors of susceptible cells and organs. These findings indicate that future studies on implications of

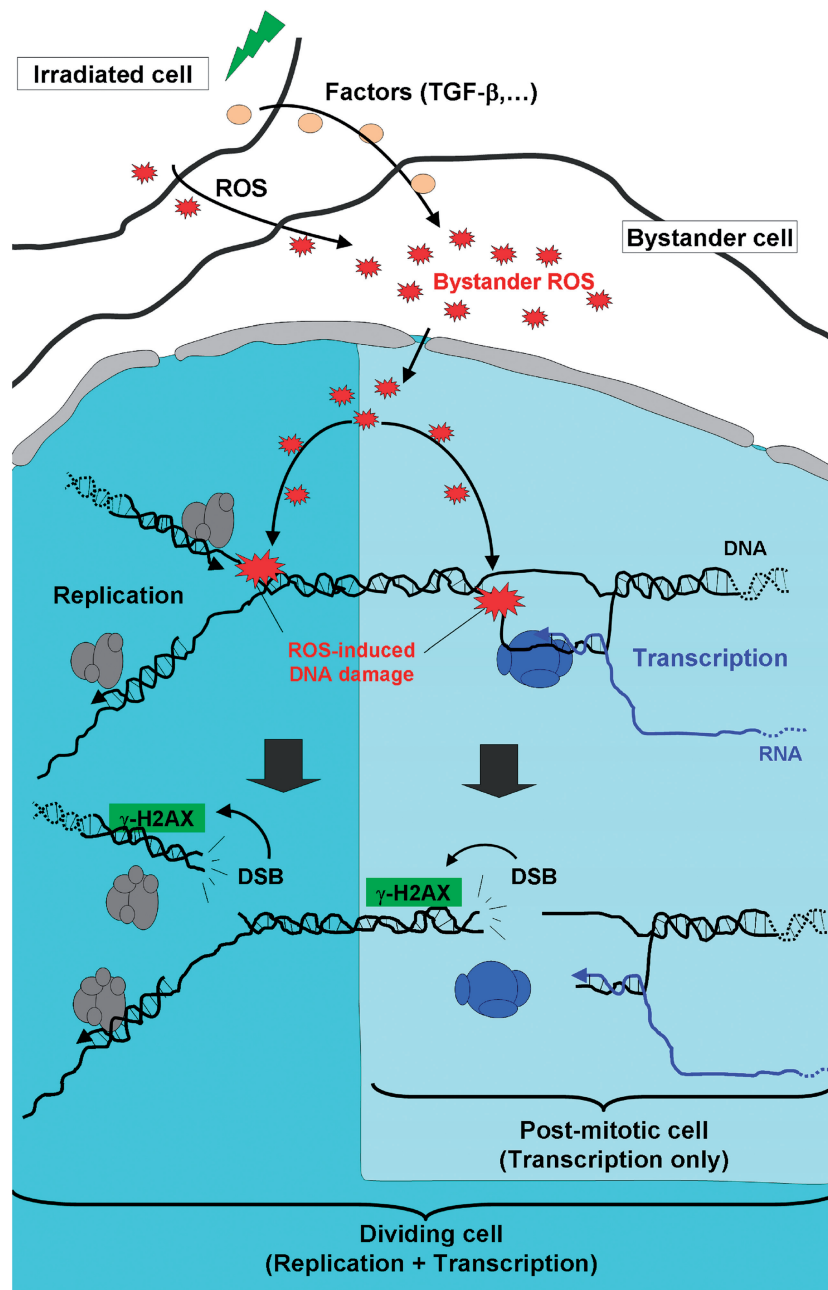


**Figure 7.** Model for DSB formation during DNA or RNA synthesis in bystander cells. Damage in irradiated cells leads to bystander effects in neighboring cells (dividing and/or non-dividing cells). Reactive oxygen species (ROS, red stars), generated directly or indirectly as a result of cell damage interact with bystander cell DNA, producing lesions ranging from base or sugar modifications to abasic sites and single-stranded breaks (large red stars). ROS-induced DNA damage can interfere with both replication and transcription in proliferating cells and transcription in non-proliferating cells, leading to DSB and  $\gamma$ -H2AX formation.

bystander effects *in vivo* should focus both on highly replicating cell types, such as those found in the gastrointestinal tract, as well as metabolically active cells including CGCs, and possibly neurons in brain regions that are subjected to excessive and/or pathological activation.

#### ACKNOWLEDGEMENTS

The authors express their appreciation to Dr V. Ashutosh Rao (FDA) for critical reading of this article.

#### FUNDING

The Intramural Funding Program of the National Cancer Institute, National Institutes of Health, USA, and the National Institute for Allergies and Infectious Disease (NIAID) Trans-NIH Biodefense Program; National Institute of Neurological Disorders and Stroke [NS056057 to A.K., in part]. Funding for open access charge: Intramural funding program of the National Cancer Institute, National Institutes of Health, USA.

*Conflict of interest statement.* None declared.

## REFERENCES

- Nagasawa, H. and Little, J.B. (1992) Induction of sister chromatid exchanges by extremely low doses of alpha-particles. *Cancer Res.*, **52**, 6394–6396.
- Prise, K.M. and O'Sullivan, J.M. (2009) Radiation-induced bystander signalling in cancer therapy. *Nat. Rev. Cancer*, **9**, 351–360.
- Blyth, B.J. and Sykes, P.J. (2011) Radiation-induced bystander effects: what are they, and how relevant are they to human radiation exposures? *Radiat. Res.*, **176**, 139–157.
- Dickey, J.S., Baird, B.J., Redon, C.E., Sokolov, M.V., Sedelnikova, O.A. and Bonner, W.M. (2009) Intercellular communication of cellular stress monitored by gamma-H2AX induction. *Carcinogenesis*, **30**, 1686–1695.
- Mothersill, C. and Seymour, C.B. (2004) Radiation-induced bystander effects—implications for cancer. *Nat. Rev. Cancer*, **4**, 158–164.
- Hei, T.K., Zhou, H., Ivanov, V.N., Hong, M., Lieberman, H.B., Brenner, D.J., Amundson, S.A. and Geard, C.R. (2008) Mechanism of radiation-induced bystander effects: a unifying model. *J. Pharm. Pharmacol.*, **60**, 943–950.
- Whiteside, J.R. and McMillan, T.J. (2009) A bystander effect is induced in human cells treated with UVA radiation but not UVB radiation. *Radiat. Res.*, **171**, 204–211.
- Morgan, W.F. (2003) Is there a common mechanism underlying genomic instability, bystander effects and other nontargeted effects of exposure to ionizing radiation? *Oncogene*, **22**, 7094–7099.
- Sedelnikova, O.A., Nakamura, A., Kovalchuk, O., Koturbash, I., Mitchell, S.A., Marino, S.A., Brenner, D.J. and Bonner, W.M. (2007) DNA double-strand breaks form in bystander cells after microbeam irradiation of three-dimensional human tissue models. *Cancer Res.*, **67**, 4295–4302.
- Sokolov, M.V., Smilenov, L.B., Hall, E.J., Panyutin, I.G., Bonner, W.M. and Sedelnikova, O.A. (2005) Ionizing radiation induces DNA double-strand breaks in bystander primary human fibroblasts. *Oncogene*, **24**, 7257–7265.
- Smilenov, L.B., Hall, E.J., Bonner, W.M. and Sedelnikova, O.A. (2006) A microbeam study of DNA double-strand breaks in bystander primary human fibroblasts. *Radiat. Prot. Dosimetry*, **122**, 256–259.
- Zhou, H., Randers-Pehrson, G., Suzuki, M., Waldren, C.A. and Hei, T.K. (2002) Genotoxic damage in non-irradiated cells: contribution from the bystander effect. *Radiat. Prot. Dosimetry*, **99**, 227–232.
- Bonner, W.M., Redon, C.E., Dickey, J.S., Nakamura, A.J., Sedelnikova, O.A., Solier, S. and Pommier, Y. (2008) gammaH2AX and cancer. *Nat. Rev. Cancer*, **8**, 957–967.
- Sedelnikova, O.A., Horikawa, I., Redon, C., Nakamura, A., Zimonjic, D.B., Popescu, N.C. and Bonner, W.M. (2008) Delayed kinetics of DNA double-strand break processing in normal and pathological aging. *Aging Cell*, **7**, 89–100.
- Hei, T.K. (2006) Cyclooxygenase-2 as a signaling molecule in radiation-induced bystander effect. *Mol. Carcinog.*, **45**, 455–460.
- Shao, C., Folkard, M. and Prise, K.M. (2008) Role of TGF-beta1 and nitric oxide in the bystander response of irradiated glioma cells. *Oncogene*, **27**, 434–440.
- Shao, C., Prise, K.M. and Folkard, M. (2008) Signaling factors for irradiated glioma cells induced bystander responses in fibroblasts. *Mutat. Res.*, **638**, 139–145.
- Shao, C., Stewart, V., Folkard, M., Michael, B.D. and Prise, K.M. (2003) Nitric oxide-mediated signaling in the bystander response of individually targeted glioma cells. *Cancer Res.*, **63**, 8437–8442.
- Mothersill, C., Rea, D., Wright, E.G., Lorimore, S.A., Murphy, D., Seymour, C.B. and O'Malley, K. (2001) Individual variation in the production of a 'bystander signal' following irradiation of primary cultures of normal human urothelium. *Carcinogenesis*, **22**, 1465–1471.
- Fournier, C., Barberet, P., Pouthier, T., Ritter, S., Fischer, B., Voss, K.O., Funayama, T., Hamada, N., Kobayashi, Y. and Taucher-Scholz, G. (2009) No evidence for DNA and early cytogenetic damage in bystander cells after heavy-ion microirradiation at two facilities. *Radiat. Res.*, **171**, 530–540.
- Burdak-Rothkamm, S., Short, S.C., Folkard, M., Rothkamm, K. and Prise, K.M. (2007) ATR-dependent radiation-induced gamma H2AX foci in bystander primary human astrocytes and glioma cells. *Oncogene*, **26**, 993–1002.
- Burhans, W.C. and Weinberger, M. (2007) DNA replication stress, genome instability and aging. *Nucleic Acids Res.*, **35**, 7545–7556.
- Burdak-Rothkamm, S., Rothkamm, K. and Prise, K.M. (2008) ATM acts downstream of ATR in the DNA damage response signaling of bystander cells. *Cancer Res.*, **68**, 7059–7065.
- Hota, S.K., Barhwal, K., Singh, S.B. and Ilavazhagan, G. (2007) Differential temporal response of hippocampus, cortex and cerebellum to hypobaric hypoxia: a biochemical approach. *Neurochem. Int.*, **51**, 384–390.
- Nicholls, D.G. (2004) Mitochondrial dysfunction and glutamate excitotoxicity studied in primary neuronal cultures. *Curr. Mol. Med.*, **4**, 149–177.
- Wu, R.S., Tsai, S. and Bonner, W.M. (1983) Changes in histone H3 composition and synthesis pattern during lymphocyte activation. *Biochemistry*, **22**, 3868–3873.
- Jakovcevska, I., Wu, J., Karl, N., Leshchynska, I., Sytnyk, V., Chen, J., Irintchev, A. and Schachner, M. (2007) Glial scar expression of CHL1, the close homolog of the adhesion molecule L1, limits recovery after spinal cord injury. *J. Neurosci.*, **27**, 7222–7233.
- Avdoshina, V., Biggio, F., Palchik, G., Campbell, L.A. and Mocchetti, I. (2010) Morphine induces the release of CCL5 from astrocytes: potential neuroprotective mechanism against the HIV protein gp120. *Glia*, **58**, 1630–1639.
- Pak, D.T., Yang, S., Rudolph-Correia, S., Kim, E. and Sheng, M. (2001) Regulation of dendritic spine morphology by SPAR, a PSD-95-associated RapGAP. *Neuron*, **31**, 289–303.
- Di Giovanni, S., Movsesyan, V., Ahmed, F., Cernak, I., Schinelli, S., Stoica, B. and Faden, A.I. (2005) Cell cycle inhibition provides neuroprotection and reduces glial proliferation and scar formation after traumatic brain injury. *Proc Natl Acad Sci USA*, **102**, 8333–8338.
- Brandoli, C., Sanna, A., De Bernardi, M.A., Follesa, P., Brooker, G. and Mocchetti, I. (1998) Brain-derived neurotrophic factor and basic fibroblast growth factor downregulate NMDA receptor function in cerebellar granule cells. *J. Neurosci.*, **18**, 7953–7961.
- Bruno, S., Giaretti, W. and Darzynkiewicz, Z. (1992) Effect of camptothecin on mitogenic stimulation of human lymphocytes: involvement of DNA topoisomerase I in cell transition from G0 to G1 phase of the cell cycle and in DNA replication. *J. Cell. Physiol.*, **151**, 478–486.
- Lois, C., Hong, E.J., Pease, S., Brown, E.J. and Baltimore, D. (2002) Germline transmission and tissue-specific expression of transgenes delivered by lentiviral vectors. *Science*, **295**, 868–872.
- Mothe, A.J., Kulbatski, I., van Bendegem, R.L., Lee, L., Kobayashi, E., Keating, A. and Tator, C.H. (2005) Analysis of green fluorescent protein expression in transgenic rats for tracking transplanted neural stem/progenitor cells. *J. Histochem. Cytochem.*, **53**, 1215–1226.
- Crowe, S.L., Movsesyan, V.A., Jorgensen, T.J. and Kondratyev, A. (2006) Rapid phosphorylation of histone H2A.X following ionotropic glutamate receptor activation. *Eur. J. Neurosci.*, **23**, 2351–2361.
- Crowe, S.L., Tsukerman, S., Gale, K., Jorgensen, T.J. and Kondratyev, A.D. (2011) Phosphorylation of histone H2A.X as an early marker of neuronal endangerment following seizures in the adult rat brain. *J. Neurosci.*, **31**, 7648–7656.
- Dickey, J.S., Baird, B.J., Redon, C.E., Sokolov, M.V., Sedelnikova, O.A. and Bonner, W.M. (2009) Intercellular communication of cellular stress monitored by {gamma}-H2AX induction. *Carcinogenesis*, **30**, 1686–1695.
- Dickey, J.S., Redon, C.E., Nakamura, A.J., Baird, B.J., Sedelnikova, O.A. and Bonner, W.M. (2009) H2AX: functional roles and potential applications. *Chromosoma*, **118**, 683–692.
- Gow, M.D., Seymour, C.B., Ryan, L.A. and Mothersill, C.E. (2010) Induction of bystander response in human glioma cells using

- high-energy electrons: a role for TGF-beta1. *Radiat. Res.*, **173**, 769–778.
40. Gerashchenko, B.I. and Howell, R.W. (2003) Flow cytometry as a strategy to study radiation-induced bystander effects in co-culture systems. *Cytometry A*, **54**, 1–7.
  41. Cleaver, J.E. (2011) gammaH2Ax: biomarker of damage or functional participant in DNA repair “all that glitters is not gold!”. *Photochem. Photobiol.*, **87**, 1230–1239.
  42. Keefer, L.K., Nims, R.W., Davies, K.M. and Wink, D.A. (1996) “NONOates” (1-substituted diazen-1-ium-1,2-diolates) as nitric oxide donors: convenient nitric oxide dosage forms. *Methods Enzymol.*, **268**, 281–293.
  43. Redon, C.E., Dickey, J.S., Nakamura, A.J., Kareva, I.G., Naf, D., Nowsheen, S., Kryston, T.B., Bonner, W.M., Georgakilas, A.G. and Sedelnikova, O.A. (2010) Tumors induce complex DNA damage in distant proliferative tissues in vivo. *Proc. Natl. Acad. Sci. USA*, **107**, 17992–17997.
  44. McKinnon, P.J. and Caldecott, K.W. (2007) DNA strand break repair and human genetic disease. *Annu. Rev. Genomics Hum. Genet.*, **8**, 37–55.
  45. Shao, C., Furusawa, Y., Aoki, M. and Ando, K. (2003) Role of gap junctional intercellular communication in radiation-induced bystander effects in human fibroblasts. *Radiat. Res.*, **160**, 318–323.
  46. Belloni, P., Latini, P. and Palitti, F. (2011) Radiation-induced bystander effect in healthy G(o) human lymphocytes: biological and clinical significance. *Mutat. Res.*, **713**, 32–38.
  47. Mancuso, M., Pasquali, E., Leonardi, S., Tanori, M., Rebessi, S., Di Majo, V., Pazzaglia, S., Toni, M.P., Pimpinella, M., Covelli, V. *et al.* (2008) Oncogenic bystander radiation effects in patched heterozygous mouse cerebellum. *Proc. Natl. Acad. Sci. USA*, **105**, 12445–12450.
  48. Baskar, R. (2010) Emerging role of radiation induced bystander effects: cell communications and carcinogenesis. *Genome Integr.*, **1**, 13.
  49. Mancuso, M., Pasquali, E., Leonardi, S., Rebessi, S., Tanori, M., Giardullo, P., Borra, F., Pazzaglia, S., Naus, C.C., Di Majo, V. *et al.* (2011) Role of connexin43 and ATP in long-range bystander radiation damage and oncogenesis in vivo. *Oncogene*, **30**, 4601–4608.
  50. Tsukimoto, M., Homma, T., Ohshima, Y. and Kojima, S. (2010) Involvement of purinergic signaling in cellular response to gamma radiation. *Radiat Res.*, **173**, 298–309.
  51. Harrison, J.F., Hollensworth, S.B., Spitz, D.R., Copeland, W.C., Wilson, G.L. and LeDoux, S.P. (2005) Oxidative stress-induced apoptosis in neurons correlates with mitochondrial DNA base excision repair pathway imbalance. *Nucleic Acids Res.*, **33**, 4660–4671.
  52. Gollapalle, E., Wang, R., Adetolu, R., Tsao, D., Francisco, D., Sigounas, G. and Georgakilas, A.G. (2007) Detection of oxidative clustered DNA lesions in X-irradiated mouse skin tissues and human MCF-7 breast cancer cells. *Radiat Res.*, **167**, 207–216.
  53. Georgakilas, A. (2011) Detection of clustered DNA lesions: biological and clinical applications. *World J. Biol. Chem.*, **2**, 173–176.
  54. McClendon, A.K. and Osheroff, N. (2007) DNA topoisomerase II, genotoxicity, and cancer. *Mutat. Res.*, **623**, 83–97.
  55. Sordet, O., Redon, C.E., Guirouilh-Barbat, J., Smith, S., Solier, S., Douarre, C., Conti, C., Nakamura, A.J., Das, B.B., Nicolas, E. *et al.* (2009) Ataxia telangiectasia mutated activation by transcription- and topoisomerase I-induced DNA double-strand breaks. *EMBO Rep.*, **10**, 887–893.
  56. Guirouilh-Barbat, J., Redon, C. and Pommier, Y. (2008) Transcription-coupled DNA double-strand breaks are mediated via the nucleotide excision repair and the Mre11-Rad50-Nbs1 complex. *Mol. Biol. Cell*, **19**, 3969–3981.
  57. Das, B.B., Antony, S., Gupta, S., Dexheimer, T.S., Redon, C.E., Garfield, S., Shiloh, Y. and Pommier, Y. (2009) Optimal function of the DNA repair enzyme TDP1 requires its phosphorylation by ATM and/or DNA-PK. *EMBO J.*, **28**, 3667–3680.
  58. Pourquier, P. and Pommier, Y. (2001) Topoisomerase I-mediated DNA damage. *Adv. Cancer Res.*, **80**, 189–216.
  59. Daroui, P., Desai, S.D., Li, T.K., Liu, A.A. and Liu, L.F. (2004) Hydrogen peroxide induces topoisomerase I-mediated DNA damage and cell death. *J. Biol. Chem.*, **279**, 14587–14594.
  60. Rass, U., Ahel, I. and West, S.C. (2007) Defective DNA repair and neurodegenerative disease. *Cell*, **130**, 991–1004.